PROCEEDINGS, 51st Workshop on Geothermal Reservoir Engineering
Stanford University, Stanford, California, February 9-11, 2026
SGP-TR-230

Assessing Geothermal Potential: A Rapid Workflow for Feasibility and Cost Analysis

William Pettitt[1], Colleen Barton[1], Elena Meyer[1], Jamar Bynum[1], Kevin McCarthy[1], Devassy Varghese[1], Wei Fu[2], Branko Damjanac[2]

[1]Baker Hughes, [2]Itasca Consulting Group

William.Pettitt@BakerHughes.com

Keywords: EGS, Reservoir Simulation, Economic Analysis

ABSTRACT

Market demand for geothermal energy is rapidly escalating globally, largely due to the need for 24/7 electrification of power grids as well as policy changes toward decarbonization and GHG (greenhouse gas) reduction. An example feasibility study is presented that focuses on viability for heat and power generation. The study applies a streamlined workflow for evaluating the feasibility of repurposing late-phase or abandoned oil and gas sites for geothermal energy production to a case study in the southern United States.

The initial phase of the workflow is Site Screening where Play Fairway Analysis (PFA) is used to down select from five areas of interest to two based on: 1) lowest risk geology; 2) highest potential heat; 3) data rich areas; 4) existing grid connections; and 5) market demand. This initial project phase includes the development of site Geomodels consisting of a structural and stratigraphic model, geomechanical model, temperature model, natural fracture assessment, and geochemistry. The initial phase incorporates the conceptual design of optimal well trajectories and stimulation zones to access the target heat source.

Steps in the second phase of the study, Pre-Feasibility, are then applied to the down-selected sites. In the second phase steps 1) fracture data are used to generate numerical Discrete Fracture Network (DFN) models; 2) hydraulic stimulations designs are stochastically developed to model hydraulic fracturing of intact rock for Enhanced Geothermal Systems (EGS) and alternatively "hydroshearing" of preexisting natural fractures; 3) the EGS and DFN models are upscaled to a gridded 3D permeability field; 4) resource potential and production forecasting of heat and minerals is performed using Reservoir Dynamic Modeling including sensitivity scenario testing of model uncertainty space; and 5) a preliminary Economic Analysis is performed which includes surface plant conceptual design, data requirements for the Basis of Design for drilling and completing the wells, drilling engineering design with risk analysis, well design time and cost estimate of DFN/EGS/AGS options, and a preliminary economic assessment for the Levelized Cost of Electricity (LCOE).

In the final study phase, Feasibility, further down selection is performed to choose the site with the highest performance capacity and lowest LCOE. The base geomodel, DFN models, and well designs, are used to conduct full-physics 3D multistage EGS stimulation modeling. In this step we simulate using Dynamic Fracture Modeling (DFM) coupled thermo-hydro-mechanical behavior of the fracture networks with 1) hydraulic fracture stimulation with no preexisting fracture network, and 2) hydraulic fracture stimulation through preexisting fracture networks to simulate reservoir injection, for production and thermal output over 30 years. The results of the full-physics-based refined DFM and Reservoir Dynamic Modeling are then used to update the techno-economic analyses.

This study presents the full link between subsurface characterization and dynamic modeling of natural and induced fracture networks to assess geothermal potential at a prospective site. We show the potential of EGS locating sites in South Texas by drilling to ~5 KM and that their relative LCOE is highly dependent on subsurface conditions. Key findings are 1) production wells must be positioned above stimulated injector to exploit the vertical growth of hydraulic fracture into regions of lower stress magnitude. 2) preexisting natural fracture networks enhance thermal output; 3) well separation has a significant impact on thermal output with respect to hydraulic fracture length distribution (or stimulation zone for natural fracture scenarios) and 4) zonal isolation ("flow conformance") significantly improves thermal output for hydraulic fracture cases.

1. INTRODUCTION

Market demand for geothermal energy is rapidly escalating globally, largely due to the need for 24/7 electrification of power grids as well as policy changes toward decarbonization and GHG (greenhouse gas) reduction. New Data Centers in North America, for example, require large-scale, isolated, continuous and secure baseload power. The Oil and Gas industry is increasingly engaged in this transition and with the application of O&G technologies to this endeavor, costs of development and investment risks are reducing due to the application of technological breakthroughs. The exploitation of deep geothermal heat is, however, difficult because it generally requires access to natural or induces fracture system that provide the permeable pathways for the extraction of geothermal fluids. By integrating technical feasibility with economic and social factors, the workflow outlines a strategic pathway for geothermal energy production, with a scalable and sustainable model for future geothermal projects.

An example feasibility study is presented that focuses on viability for heat and power generation. The initial phase of workflow is Site Screening where Play Fairway Analysis was used to down select from five areas of interest to two based on: 1) lowest risk geology; 2) highest potential heat; 3) data rich areas; 4) existing grid connections; 5) market demand (McCarthy, 2024). This initial project phase includes the development of site Geomodels consisting of a structural and stratigraphic model, geomechanical model, temperature model, natural fracture assessment, and geochemistry. Steps in the second phase of the study, Pre-Feasibility, were then applied to the two down-selected sites: 1) fracture data are used to generate numerical Discrete Fracture Network (DFN) models; 2) hydraulic stimulations designs to model hydraulic fracturing of intact rock or Enhanced Geothermal Systems (EGS) and/or "hydroshearing" of preexisting natural fractures; 3) the EGS and DFN models are upscaled to a gridded 3D permeability field; 4) resource potential and production forecasting of heat & minerals is performed using Reservoir Dynamic Modeling including sensitivity scenario testing of model uncertainty space; and 5) a preliminary Economic Analysis is performed which includes surface plant conceptual design, data requirements for the Basis of Design for drilling and completing the wells, drilling engineering design with risk analysis, well design time and cost estimate of DFN/EGS/AGS options, and a preliminary economic assessment for the Levelized Cost of Electricity (LCOE). The final study phase is the Economic Analysis which includes: 1) surface plant conceptual design; 2) data requirements for well Basis of Design for drilling and completing the wells; 3) drilling engineering design with risk analysis, 4) well design time and cost estimate for DFN and EGS options; 5) economic assessment for Levelized Cost of Electricity (LCOE).

In the final study phase, Feasibility, further down selection is performed to choose the site with the highest performance capacity and lowest LCOE. The base geomodel, DFN models, and well designs, are used to conduct full-physics 3D multistage EGS stimulation modeling. In this step we simulate coupled thermo-hydro-mechanical behavior of the fracture networks with 1) hydraulic fracture stimulation with no preexisting fracture network, and 2) hydraulic fracture stimulation through preexisting fracture networks to simulate reservoir injection, production and thermal output over 30 years. The results of the full-physics based refined Reservoir Dynamic Modeling is then used to update the techno-economic analyses.

2. PHASE 1 — SITE CHARACTERIZATION

2.1 Geomodels

Site specific thermal data for Site 1 was derived from Batir and Richards (2020) and that of Site 2 from Blackwell et al. (2011) with temperatures calibrated against well-based temperature log measurements. Examples of the regional to site specific temperature modeling a shown in Figure 1. Log profiles through the temperature volume are shown in Figure 2. Target temperatures for the study were 220°C-230°C. To develop the structural and stratigraphic models for each site formation tops and structural horizons were based on available log data at shallower depths. Depth to basement for Site 1 was sourced from Blackwell et al. (2011).

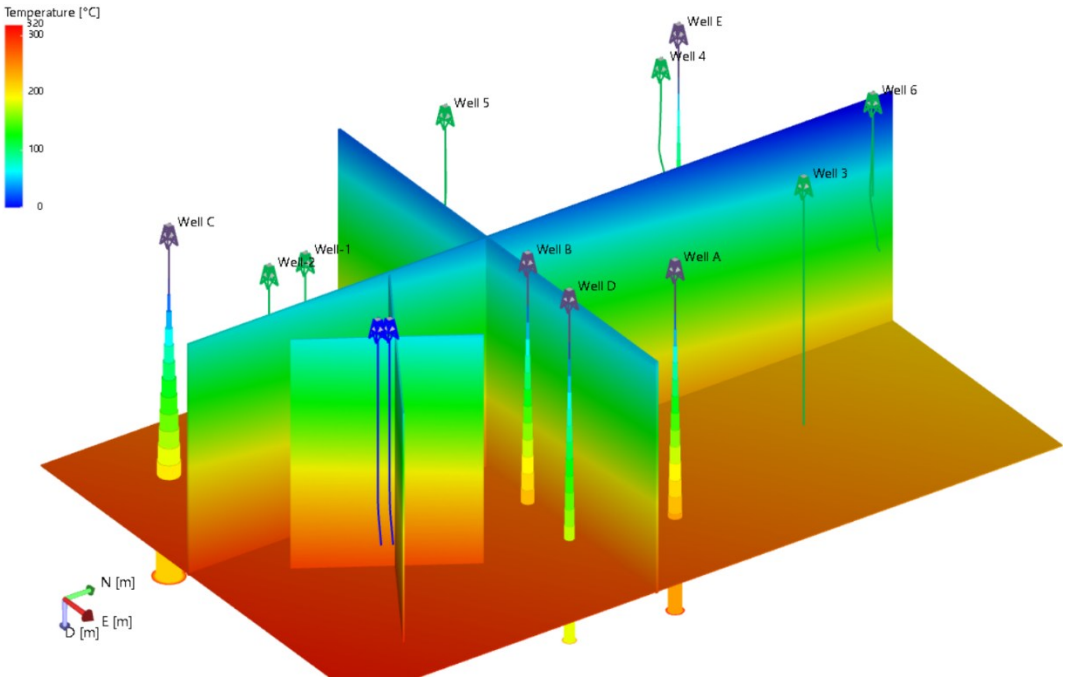

Figure 1: Temperature model example for Site 1. Regional-scale temperature horizons were calibrated with well log temperature profiles.

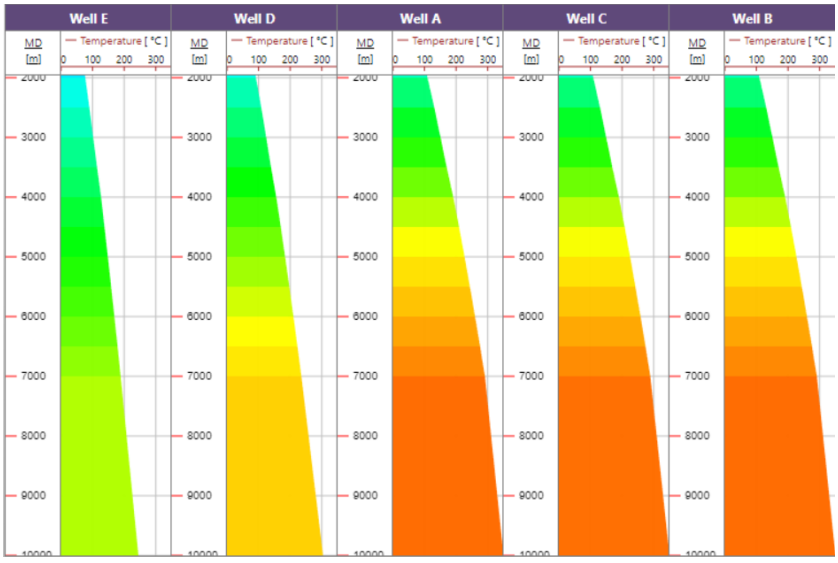

Figure 2: Logs constructed through the temperature volume demonstrate temperature variation across Site 1.

3D Geomechanical models were developed for both sites through analysis of log data acquired in study wells to constrain the pore pressure, stress field, and rock geomechanical properties as a function of depth. Bulk density logs were used to model the overburden stress. Additional key parameters required for site screening are thermal conductivity and matrix permeability. For required values below measured log depths, value ranges were drawn from available literature for each site. Figure 3 summarizes these parameters for the Site 1 Case.

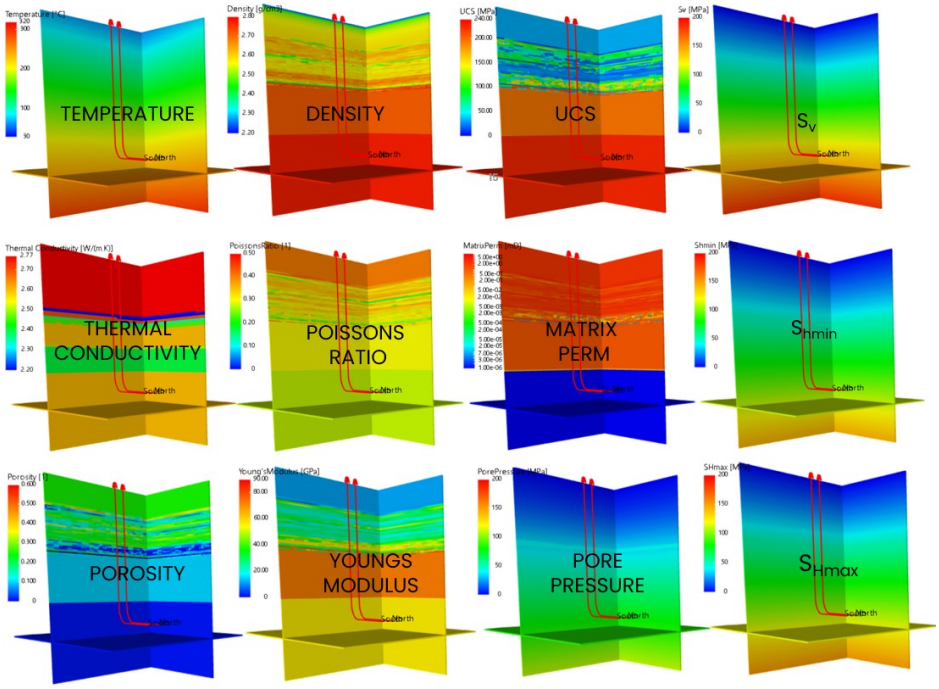

Figure 3: Geomechanics and thermal properties required for dynamic reservoir modeling. Example from Site 1.

2.2 Well Basis of Design

Three basic Class 5 well configurations were used for the various study simulations and economic analyses (Figure 4). For the pre-feasibility DFN cases these configurations were employed in two scenarios; one, a doublet of lateral wells of approximately 1,000 m lateral length located 300 m apart at the same depth and the other, a vertical injector perforated 250 m above a lateral producer. In the pre-feasibility EGS cases the wells were again doublets of lateral injector/producer pairs of approximately 1,000 m lateral length located 300

m apart at the same depth. In the feasibility case scenarios, lateral injectors remained at fix depth and producers were placed 150m, 200m, or 250m above the injector. In all cases the injectors are modeled as perforated and stimulated and the producers as open hole completions.

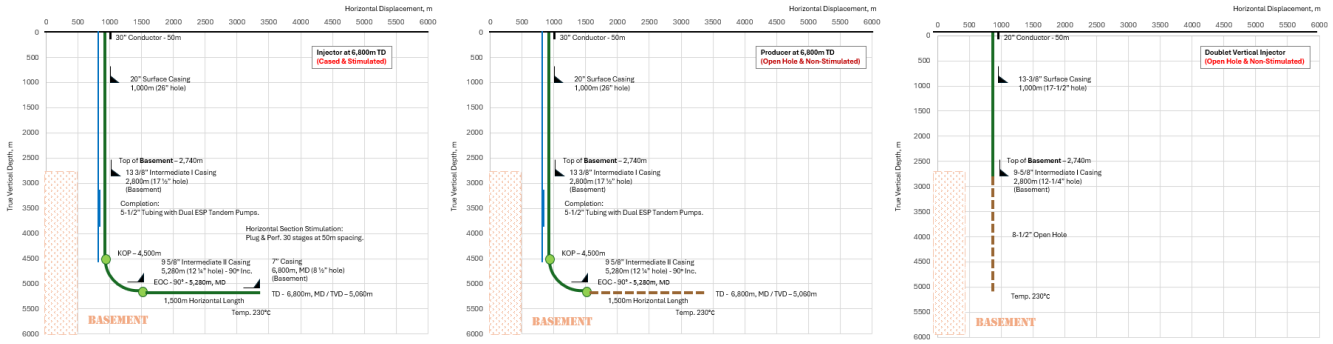

Figure 4: Well configurations applied in model cases.

3. PHASE 2 — PRE FEASIBILITY

3.1 DFN Fracture Modeling

For DFN systems, natural fracture networks were simulated to optimize hydrothermal fluid flow. We use a finite element software that employs the hydro-structural approach of DFN model generation. This approach involves analysis and modeling that explicitly incorporates the geometry and other properties of discrete features as a central component controlling flow and transport. In these DFN models, a stochastic 'pipe' network-type algorithm is used to calculate flow and transport through the fracture network. Although no site-specific log-based natural fracture data were available for these sites, the stochastic distributions of fracture geometries were divided into three sets consistent with fracture analyses of more regional fracture trends in the lithologies modeled (Ferrill and Ferrill, 2021). The fracture sets were spatially modeled by Poisson distributions.

Stress aperture coupling facilitates the analysis of the sensitivity of natural fractures or faults to in situ stress that can be used to optimize well design and thereby enhance production. The stress-aperture coupling within this study uses the compliance model of Moos and Barton (2008) also detailed in Barton et al. (2025). This stress-permeability coupling is dynamically computed during DFN model development. Transmissivities within the range of 1.0E-01 to 1.0E-07 m2/s were used in the models. Dense, moderate and sparse fracture DFN intensities were generated to assess uncertainties in the natural fracture characterization at the study sites. Figure 5 provides an example of the full stochastic DFN model for the Site 1 case left, and right, a slice through this model at the depth of the lateral wells.

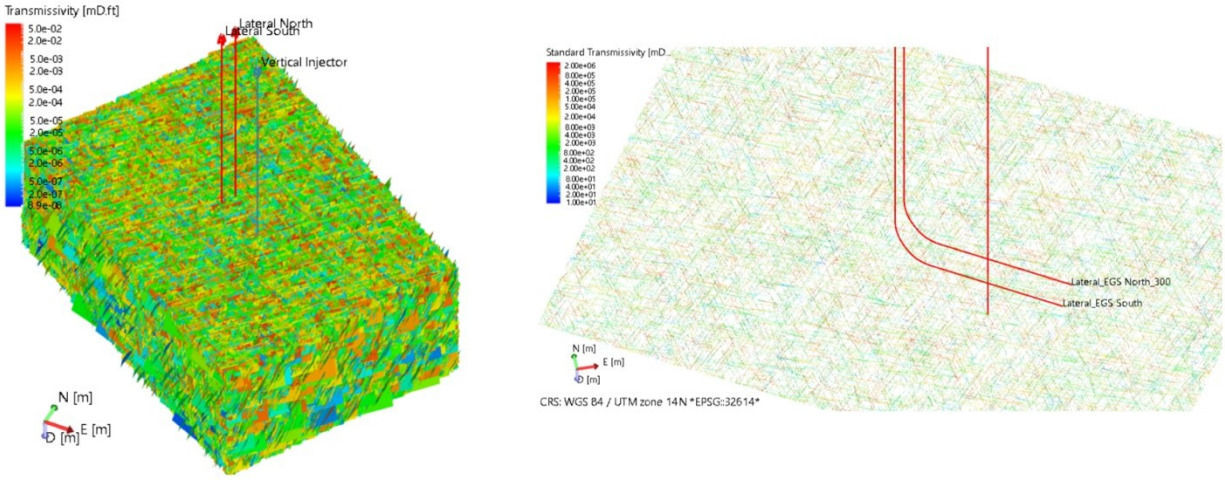

Figure 5: Full stochastic DFN model for the Site 1 case (left) and slice through this model at the depth of the lateral wells (right).

To model flow and transport on the regional scale over time, the properties of a network of discrete fractures of lengths less than the continuum grid blocks are upscaled into the geomodel grid (Figure 6). Model grids with 75m in X, 75m in Y with variable vertical cell

thickness were built from the surface to the mid-Basement for each site at a depth of approximately 5,060 m Site 1 and 5440 m for Site2 to accommodate DFN upscaling. The resulting upscaled parameters are a directional hydraulic conductivity tensor, fracture kinematic porosity, and other transport properties. A flux-based upscaling method is used that requires several flow calculations through a DFN model calculated for each head gradient direction. The hydraulic conductivity tensor is then derived by a least-squares fit to these flux responses for the fixed head gradients. the Kx, Ky, Kz permeabilities of the base DFN model for Site 1 are shown in Figure 6. The upscaled permeabilities range from 10E-06 to 5.0E+02 mD. These DFN-derived fracture permeability distributions were used in dynamic fluid modeling to explore well engineering scenarios for optimal production including well designs of both lateral doublets spaced at 300 m and vertical and lateral doublets (Figure 6).

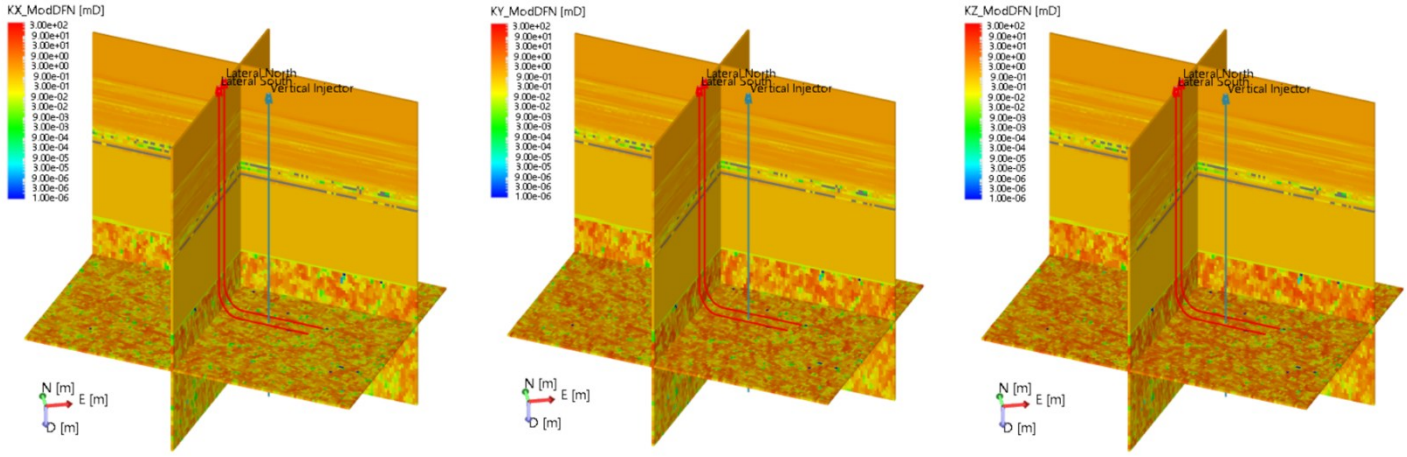

Figure 6: Upscaled directional hydraulic conductivity tensor of the DFN fractur network

3.2 EGS Fracture Modeling

The EGS conceptual model is based on recent EGS field experimental studies undertaken through the U.S. DOE FORGE project in Utah and applied at the Blue Mountain field in Northern Nevada (Norbeck et al., 2024). These studies are conducted at significant depths in granite host rock with lateral injector producer well doublet designs. The technologies applied in these studies are those developed for the oil and gas industry hydraulic fracturing operations where lateral wells are drilled parallel to the direction of least horizontal stress, cased, and perforated at specific cluster spacings.

EGS scenarios employed stochastic modeling to represent hydraulic stimulation and perforation clusters, bypassing computationally intensive fracture propagation simulations. A refined geomodel grid was built with 10m X 10m X 10m cell dimensions to provide the high resolution required to capture well-to-well dynamic flow as a result of enhanced permeability around stimulated zones. Parallel doublet EGS wells of approximately 1,500 m lateral length located 300 m apart were designed for this phase of the modeling study (Figure 7).

In the Pre-Feasibility phase, a stochastic approach was used to represent perforation clusters (“perfs”) along the lateral wells. Numerous cluster spacings, fracture sizes, and stochastic approaches were tested. This iterative approach revealed that clusters spacing is a strong factor controlling residence time of fluid flow through the fractures to optimize heat extraction and minimize heat depletion. Both uniform and non-uniform clusters cluster spacings were modeled to approximate stress shadow effects. Fracture half-lengths were varied between 125 and 155m and hydraulic apertures between 5.0E-5mm and 1.0E-05mm were used. Fracture intensity was varied from sparse to dense by varying cluster spacing between 30-50m per cluster and 3-7 perforations per cluster. These statistical approaches were designed to mimic the variability in fracture propagation commonly experienced in hydraulic fracturing operations. Figure 7 presents the geometry typical explicit perf distributions applied in this study located within the full DFN model.

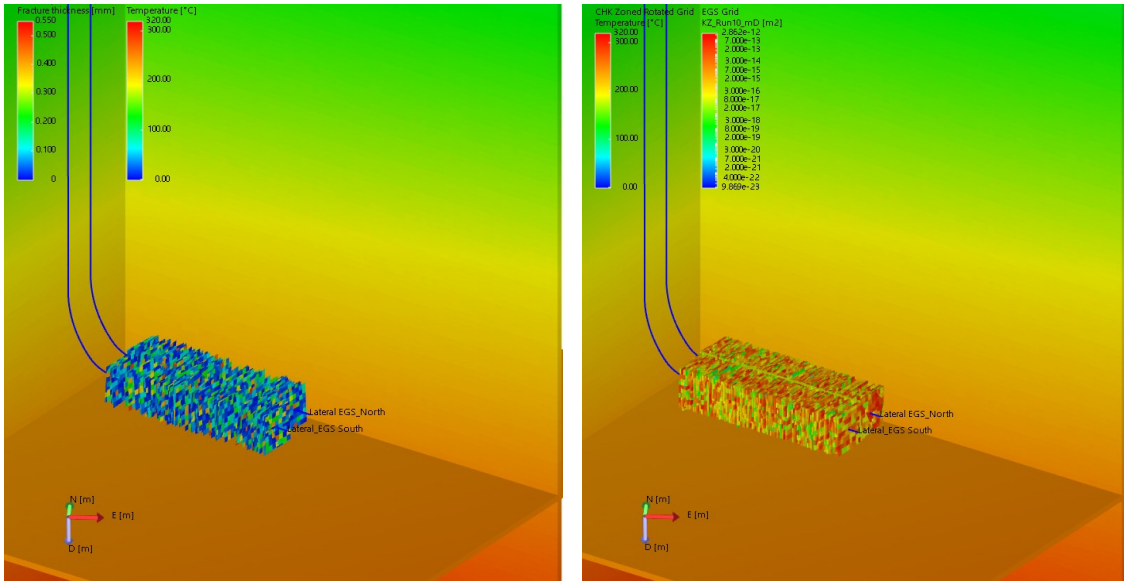

Figure 7: Geometry of explicitly generated perforation clusters applied in this study located within the model area Hydraulic aperture (left), Kz permeability (right).

3.3 Reservoir Simulation

3.3.1 DFN Forecast Models

The JewelSuite 3D static geomodel grid was exported via a RESCUE file format and incorporated into a commercial reservoir simulator for the dynamic reservoir modeling study. Three separate DFN permeability cases were simulated for dense, moderate, and sparse fracture intensity models. For each of these three cases, two scenarios were simulated — two lateral wells separated by 300m and 2) a lateral and a vertical injector 250m above a lateral producer. In addition to these 12 separate scenarios, for each of the three model cases, sensitivity tests were performed varying target injection rate and maximum drawdown.

An example of the reservoir permeability and corresponding temperature at the end of 30 years production of the lateral well doublet scenario is shown in Figure 8 and that of the vertical injector – lateral producer doublet in Figure 9 for the Site 1 case. For both sites, dynamic modeling results indicate dense DFN cases outperform cases with lower fracture intensity as expected for both sites. The optimal drawdown target was established to be 75kg/s for all cases for both site cases, however the optimal maximum drawdown was modeled to be less for the Site 2 case than Site 1 likely due to difference in underlying rock properties of matrix permeability and porosity between the granite of Site 1 and the mix of carbonate and sandstone lithologies of Site 2. The thermal output over 30 years for the two sets of well doublet cases for the two sites are compared in Figure 10 showing less than 10% decline over 30 years.

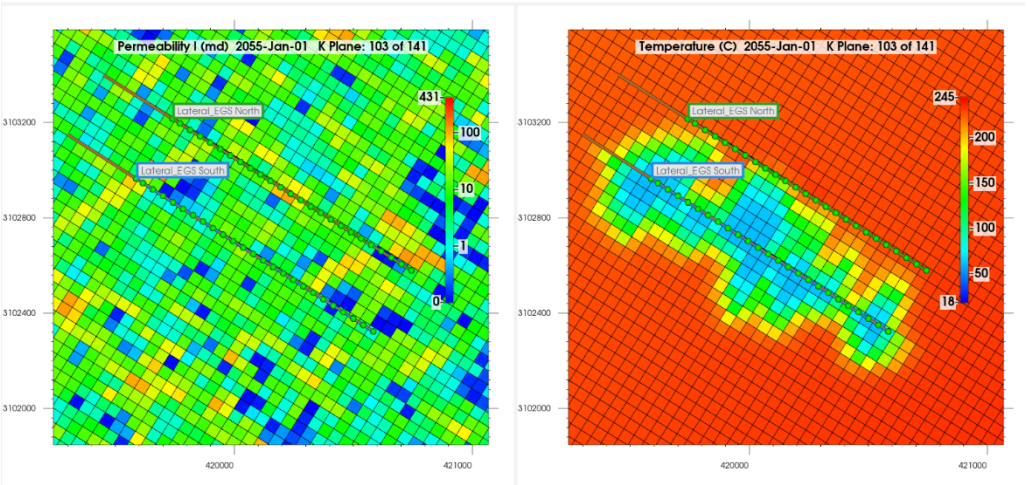

Figure 8: Reservoir permeability and corresponding temperature at the end of 30 years production for the DFN case of lateral wells doublet scenario.

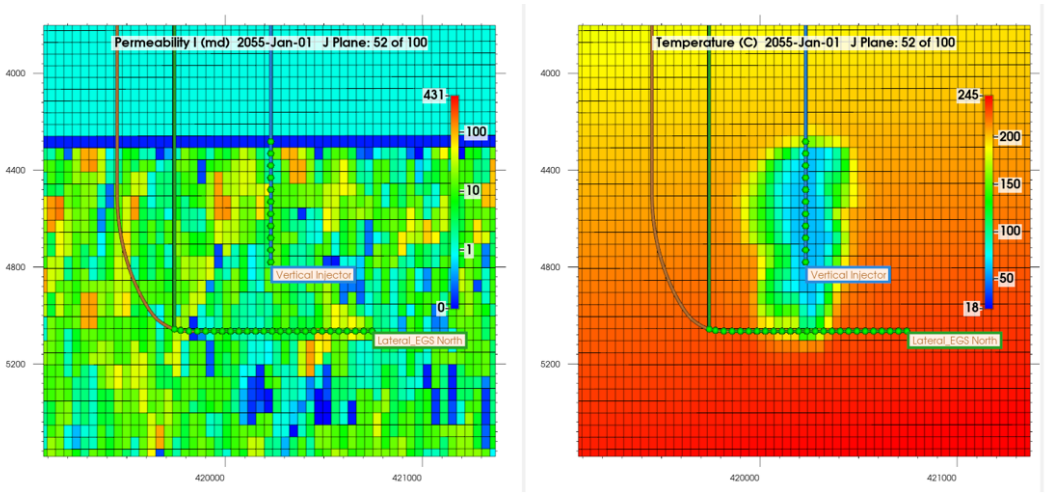

Figure 9: Reservoir permeability and corresponding temperature at the end of 30 years production for the DFN case of a vertical/lateral well doublet scenario.

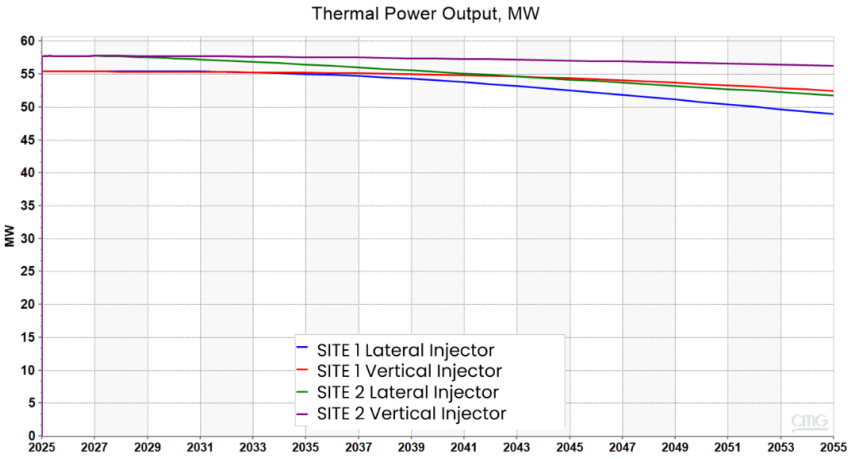

Figure 10: Thermal output over 30 years for the pre-feasibility DFN cases for the two sites.

3.3.2 EGS Forecast Models

Various simulation cases of hydraulic fracture perforation clusters along the laterals were modeled using the statistical approach discussed above. This iterative modeling process included simulations over a range of hydraulic fracture cluster spacings, perforations per cluster, fracture half-lengths and fracture propagation uniformity. Dynamic reservoir modeling simulation sensitivity analyses tested a range of drawdown pressures and target injection rates. All simulations were run with a horizontal injector located 300m from the producer at the corresponding depth. The optimal configuration for both sites was a uniform, dense clusters spacing at 30 m with 7 clusters/stage and 150m fracture half-length.

Figure 11 provides an example of reservoir permeability and corresponding temperature at the end of 30 years production of the lateral well doublet scenario for the Site 1 case. The thermal output for both sites is similar when the same target injection rates are applied in spite of the difference in rock properties (Figure 12). For these hydraulic fracture cases modeling at the target depths for the two sites there is a 30-45% decline over 30 years.

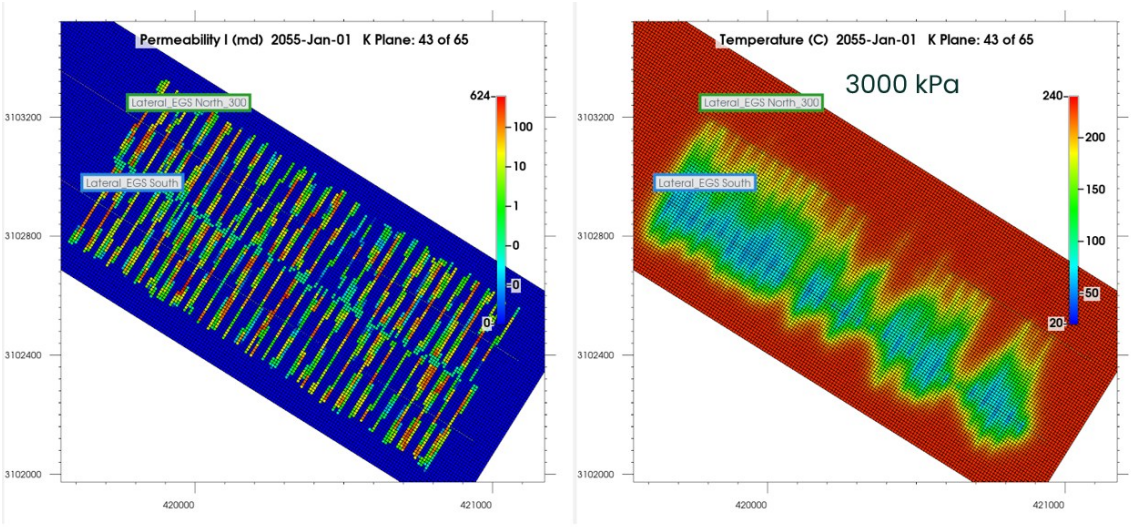

Figure 11: Reservoir permeability and corresponding temperature at the end of 30 years production of the lateral well doublet scenario for the Site 1 EGS case.

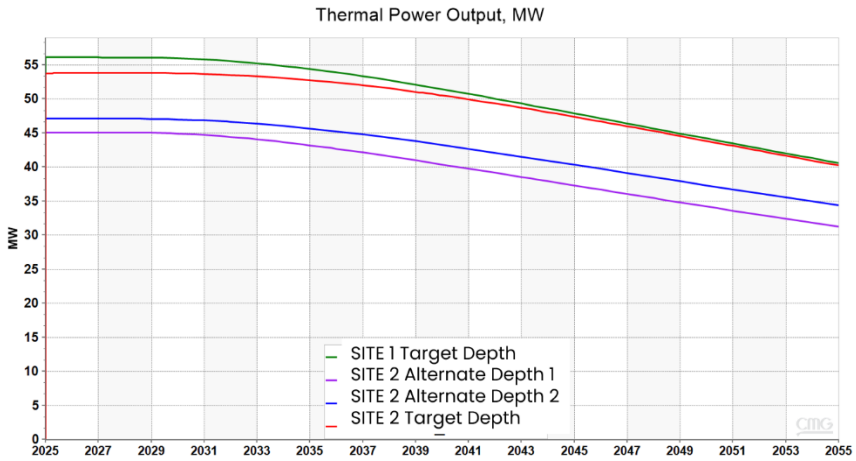

Figure 12: Thermal output for the pre-feasibility hydraulic fracture cases for both Site 1 and Site 2 over thirty years.

3.4 Pre-Feasibility Economic Analysis

A pre-feasibility economic assessment of the selected geothermal development options has been conducted to calculate the Levelized Cost of Electricity (LCOE) and Unit Overnight Capital Cost (OCC). The assessment is based on the various economic and commercial assumptions described herein.

LCOE is a measure of the discounted lifetime cost of building and operating an electricity generating asset. It is specified in $/kWh or $/MWh and includes all relevant costs faced by a developer such as exploration & drilling costs, capital, operating and maintenance(O&M), decommissioning, financing etc. and is used to compare different electricity generation technologies and development scenarios.

The formula for calculating LCOE is as follows:

$$LCOE = \frac{\sum_n \frac{Total\ Costs}{(1+r)^n}}{\sum_n \frac{Total\ Electricity\ Generated}{(1+r)^n}}$$

Where n = time-period, r = discount rate

OCC refers to the estimate of construction costs if the project is completed overnight. It is a simplistic metric for comparing unit upfront costs between development scenarios and specified in $/kW. Compared to LCOE, OCC excludes considerations of interest on debt, discount rate, capacity factor, project term, etc.

The formula for calculating OCC is as follows:

$$Unit\ OCC = \frac{Overnight\ Construction\ Costs}{NamePlate\ Power\ Capacity}$$

The technical cases given in Table 1, and described in previous sections, were evaluated for their LCOE and other economic metrics.

Table 1: Pre-Feasibility Cases for Economic Analysis

Site	Case	Technical Case
1	1	DFN Vertical Injector
1	2	DFN Lateral Injector
1	3	EGS Target Depth
2	1	DFN Vertical Injector
2	2	DFN Lateral Injector
2	3	EGS Depth 1
2	4	EGS Depth 2
2	5	EGS Target Depth

For each development case, the project concept consists of a geothermal well doublet (producer, injector) and an Organic Rankine Cycle (ORC) Power Plant that converts thermal heat to electricity. The CAPEX costs include E&A costs, Well Costs, Stimulation, Power Plant Costs, Field Gathering Systems. The OPEX costs include Well O&M, Plant O&M, Labor Costs, Water O&M and Pumping.

The following base case assumptions were used in the economic model:

- All calculations are performed in US$ and in Nominal (money of the day) terms.
- Inflation Assumptions:
    - CAPEX Inflation: 2%
    - OPEX Inflation: 5% (Avg. based on historic 10-year CPI in southern US)
    - Derisking phase estimated to last 2 years.
- Exploration & Appraisal costs (derisking phase) are estimated to be in the range of US$15MM – US$24MM. Average of the range (US$19MM) used in LCOE calculation.
- Upfront construction assumed to be scheduled over two years (Yr3 25%, Yr4 75%)
- Power Plant & Other Capex: Estimated based on correlation in comparable project data. Internal Baker Hughes project data intelligence and publicly available literature used. Includes cost of field gathering systems, indirect costs and contingency.
- O&M costs: Estimated based on internal BH project data intelligence and publicly available literature.
- Costs have been estimated based on US and other global examples. Site-specific cost location factors applied are as follows:
    - Well Capex: 100% (US procurement assumed)
    - Power Plant Capex: 90% (average of equipment procured and local sourcing)
    - OPEX: 85% (mostly operations and maintenance using local resources)
    - Decommissioning Costs: 15% of capex estimate
    - Availability Factor: 90% (to account for parasitic load)
    - Operating Term: 25 years of production
    - Project Financing: 0% (unlevered basis)
    - Discount rate (Nominal): 9.00%

The relative Levelized Cost of Electricity (LCOE) values calculated using base case assumptions are shown in Figure 13. LCOE ranges are lowest for the DFN cases and somewhat higher for the EGS cases. The wider variation in EGS cases is due to the steep decline in thermal output and stimulation expenses in certain cases. Figure 14 is a cost percent breakdown of the components of the LCOE.

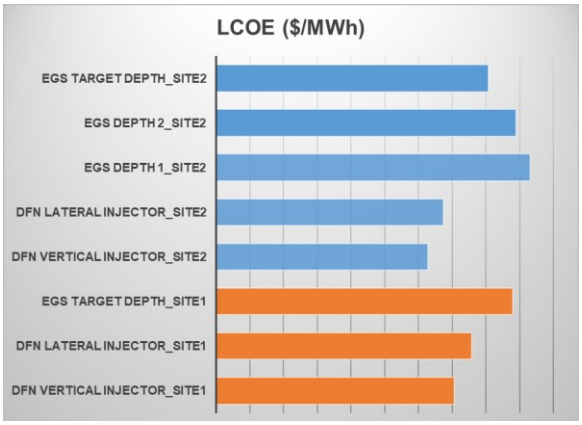

Figure 13: Comparison of the relative Levelized Cost of Electricity (LCOE) for all study scenarios. Site 1 is Orange, Site 2 Blue.

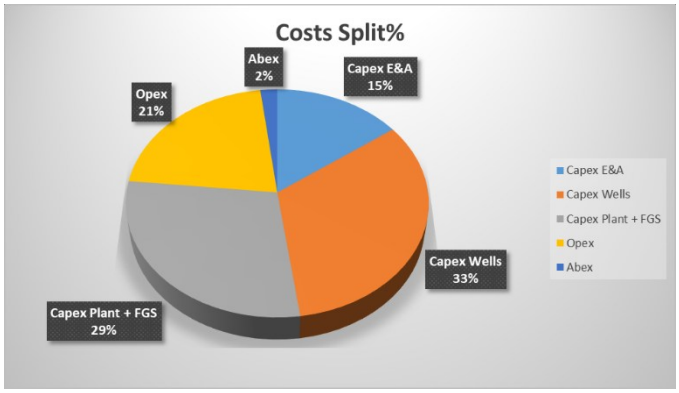

Figure 14: Cost split breakdown of the CAPEX and OPEX components of the Levelized Cost of Electricity (LCOE)

4. PHASE 3 — FEASIBILITY

4.1 DFM Modeling

Enhancing the geothermal system through hydroshearing/hydraulic stimulation is simulated by Dynamic Fracture Modeling (DFM) through the natural fracture network and, alternatively, through hydraulic fracture modeling in the absence of natural fractures. The DFM modeling was carried out using numerical software XSite, which uses the lattice approach to implement the synthetic rock mass (SRM) method for simulation of hydraulic fracturing with or without naturally fractured rock masses (Damjanac et al., 2021). The XSite software has the capability to model both near-wellbore effects and field-scale reservoir stimulation, including complex fracture initiation and propagation. Fully coupled thermo-hydro-mechanical simulation is conducted in the model that explicitly represents pre-existing fractures. Reservoir stimulation is a combination of hydraulic fracture propagation and opening or shear of pre-existing joints (i.e., hydro-shearing). The DFN/DFM and DFM-derived fracture permeability distributions were then used in dynamic fluid modeling to explore well engineering scenarios for optimal production over 30 years. The model geometry in both cases is 60 m long stages for 13 stages totaling ~800 m. and slickwater injection for 1.1 hour per stage. The producer and injectors are both modeled as lateral wells. The injector is 7" cased with a plug-and-perf completion, and the producer is modeled as a 9 5/8" open-hole completion. We designed and implemented a "zonal isolation model" into the reservoir modeling to assess flow conformance and performed sensitivity tests for 1) well separation, 2) zonal isolation and3) the presence or absence of natural fractures.

The pure hydraulic fracturing case in the absence of natural fractures yields the growth of 2~3 relatively isolated fractures per stage with predominantly upward growth affected by stress shadowing effects. Figure 15 presents the stage-by-stage hydraulic fractures along the lateral injector (left) and the resulting hydraulic aperture contoured on the fracture surfaces (right). In this case, where the granite is assumed to be massive such that fracture growth is not contained, the dominant upward fracture growth clearly dictates that production wells must be positioned above the stimulated injector to exploit the vertical growth of hydraulic fracture into regions of lower stress magnitude. Stacking wells vertically maximizes the effectiveness of the hydraulic stimulation.

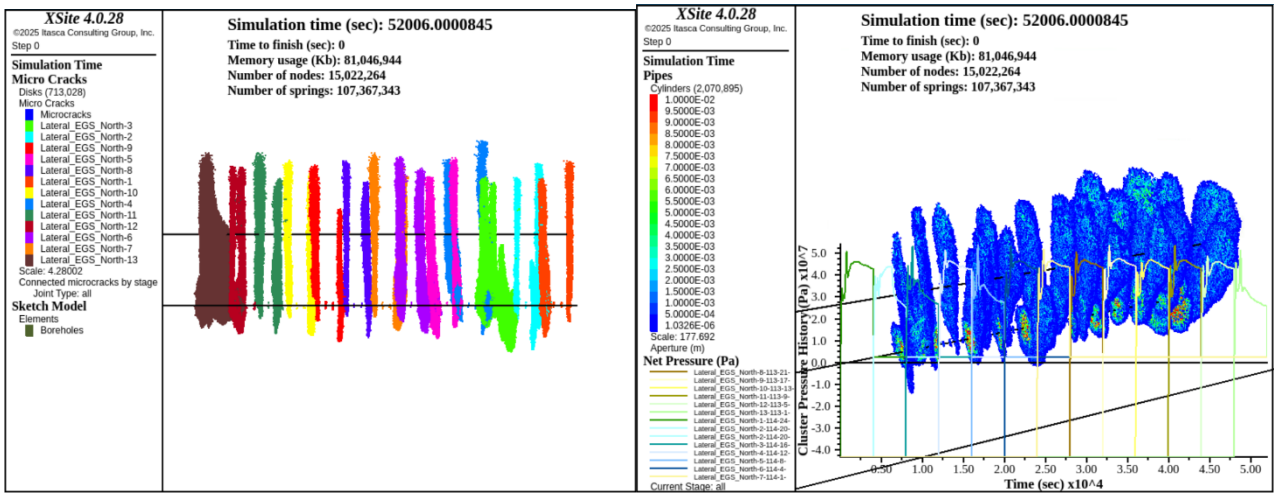

Figure 15. Stage-by-stage hydraulic fractures along the lateral injector (left) and the resulting hydraulic aperture across the hydraulic fracture face (right).). Note that the horizontal black line at the base of the fractures denotes the injection well.

Hydraulic fracturing of a naturally fractured reservoir yields a more complex fracture propagation path due to the effect of natural fractures. For most stages there was less upward growth of the discrete hydraulic fractures due to their arrest after intersection with preexisting natural fractures. For some stages, natural fracture stimulation extends over greater distances due to flow pathways provided by subvertical natural fractures or by hydraulic fractures growing into stimulated fractures. Figure 16 presents the stage-by-stage stimulation of fractures along the lateral injector (left) and the resulting hydraulic aperture contoured on the hydraulic fracture surfaces (right). Although upward fracture propagation is still dominant, there is significant downward fracture growth due to the activation of preexisting natural fractures.

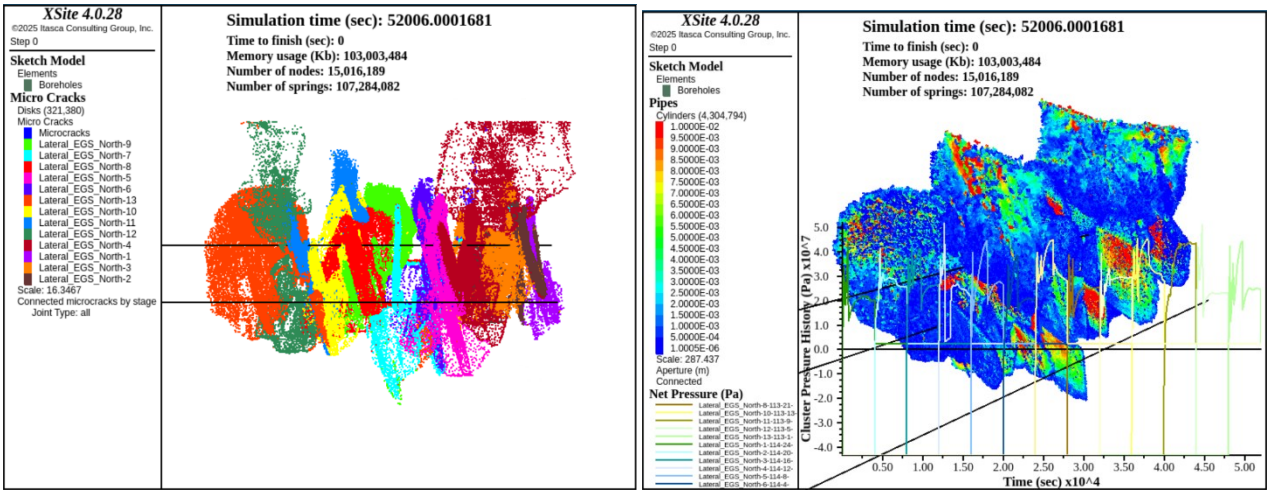

Figure 16. Stage-by-stage stimulation of fractures along the lateral injector (left) and the resulting hydraulic aperture across the hydraulic fracture face (right). Note that the horizontal black line at the base of the fractures denotes the injection well.

It has been demonstrated analytically that successful EGS development requires fracture stimulation that provides a large amount of surface area for thermal convection coupled with a relatively low flow rates within the stimulated volume to sustain viable thermal output (Doe et al., 2014). The full physics coupled thermo-hydro-mechanical simulation applied in this study verifies this requirement simulating near-wellbore fracture initiation and propagation that includes perforation effects, stress interference, and proppant transport and placement. dynamic reservoir modeling of flow through these complex fracture shows that flow rates at a few specific perforations can dominate flow and quickly short-circuit potential flow paths leading to non-uniform flow along the injector and rapid thermal breakthrough (Figure 17). Flow conformance is operationally achieved in the Oil and Gas industry through Inflow Control Devices (ICDs). In this study this zonal isolation was implemented by shutting in perforations that exceeded a prescribed flow rate (~ 150 m3/day) to equalize the flow along the wellbore and ensure more distributed flow, higher residence time, greater heat production, and to delay thermal breakthrough.

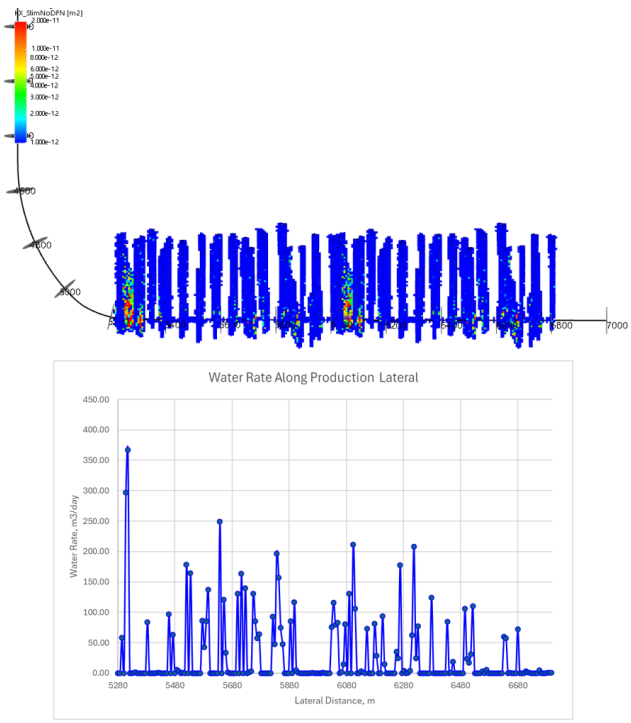

Figure 17. Dynamic reservoir modeling of flow through complex hydraulic fractures shows that flow rates at a few specific perforations can dominate flow.

4.2 DFM Forecast Modeling

Sensitivity tests were simulated to assess the optimal separation of the producer above the injector for stimulation in both massive granite and naturally fractured granite. Well separations modeled are 150m, 200m and 250m. Eash of these cases was modeled with and without zonal isolation.

Figure 18 shows reservoir temperature in the volume after 30 years of production for the sequence of increasing well separation for the hydraulic fracture only case with no zonal isolation. Figure 19 presents the decline curves over 30 years of production. The optimal well separation of the three cases is 250 m. However, there is a 20% thermal decline over 10 years and a 55% thermal decline after 30 years of production.

Figure 20 shows reservoir temperature in the volume after 30 years of production for the sequence of increasing well separation for the hydrofrac only case with zonal isolation. Figure 21 presents the decline curves over 30 years of production. The optimal well separation of the three cases is 250 m, and with zonal isolation there is a 9% thermal decline over 10 years and a 40% thermal decline after 30 years of production.

Figure 22 shows reservoir temperature in the volume after 30 years of production for the sequence of increasing well separation for the case of hydraulic fracture propagation within a preexisting natural fracture network without zonal isolation. Figure 23 presents the decline curves over 30 years of production. The optimal well separation of the three cases is 250 m, and without zonal isolation there is an 8% thermal decline over 10 years and a 25% thermal decline after 30 years of production.

Figure 24 shows reservoir temperature in the volume after 30 years of production for the sequence of increasing well separation for the case for hydraulic fracture propagation within a preexisting natural fracture network with zonal isolation. Figure 25 presents the decline curves over 30 years of production. The optimal well separation of the three cases is 250 m, and with zonal isolation there is a 7% thermal decline over 10 years and a 25% thermal decline after 30 years of production.

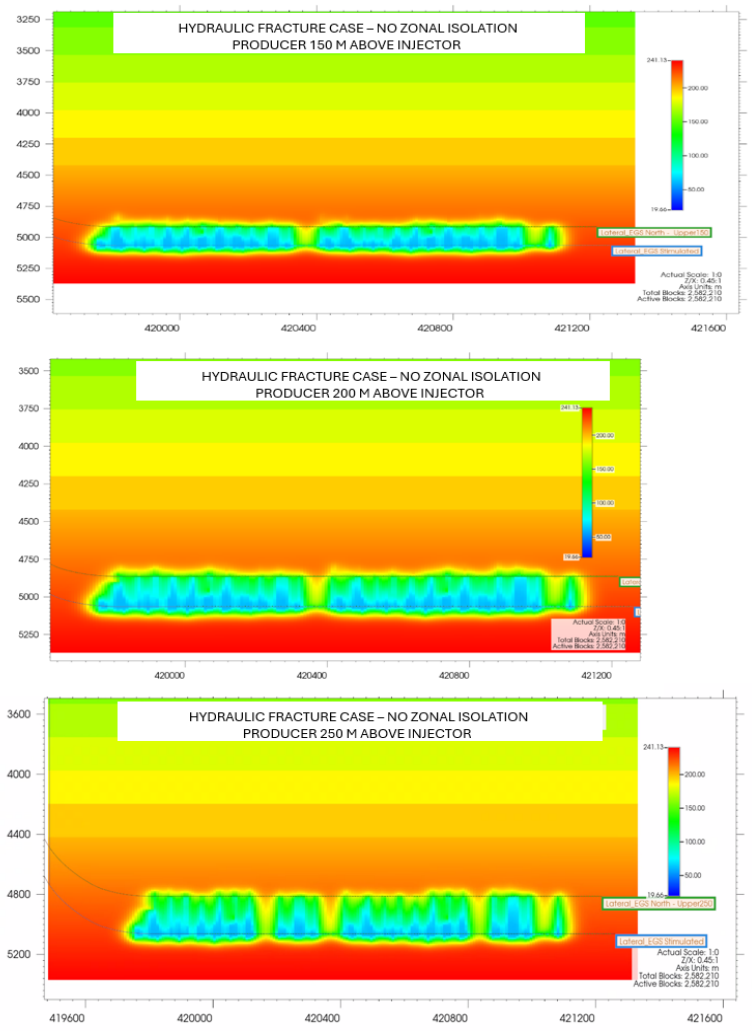

Figure 18. Reservoir temperature in the volume after 30 years of production for the hydrofrac only case without zonal isolation.

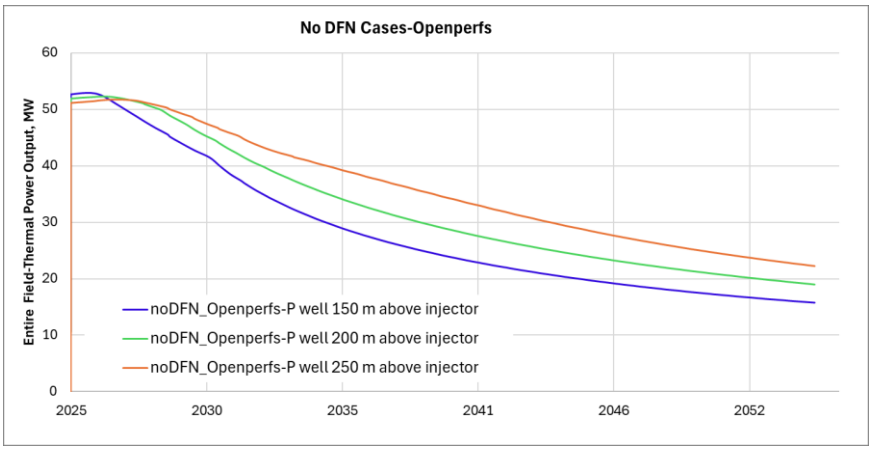

Figure 19. Decline curves over 30 years of production for the hydrofrac only case without zonal isolation.

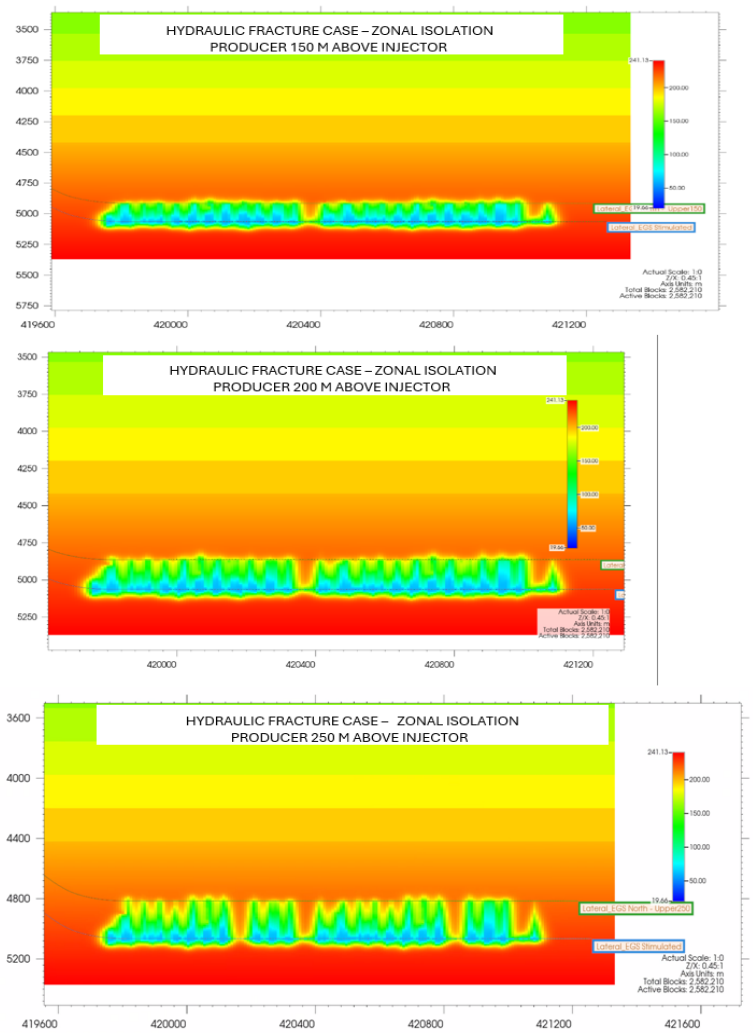

Figure 20. Reservoir temperature in the volume after 30 years of production for the hydrofrac only case with zonal isolation.

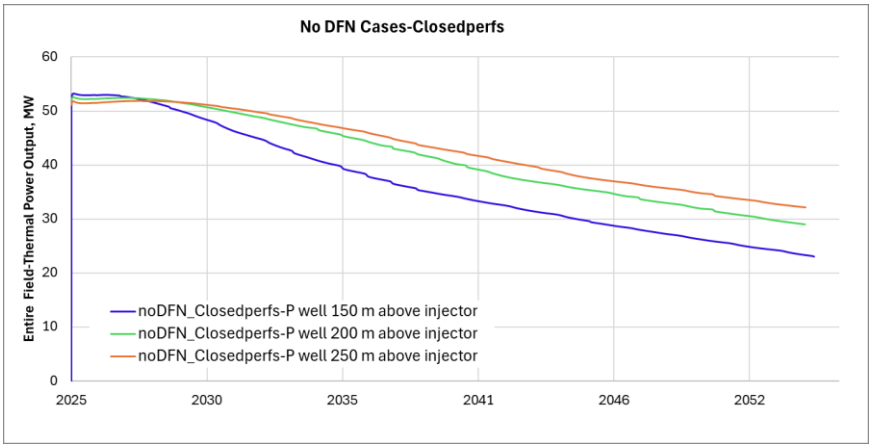

Figure 21. Decline curves over 30 years of production for the hydrofrac only case with zonal isolation.

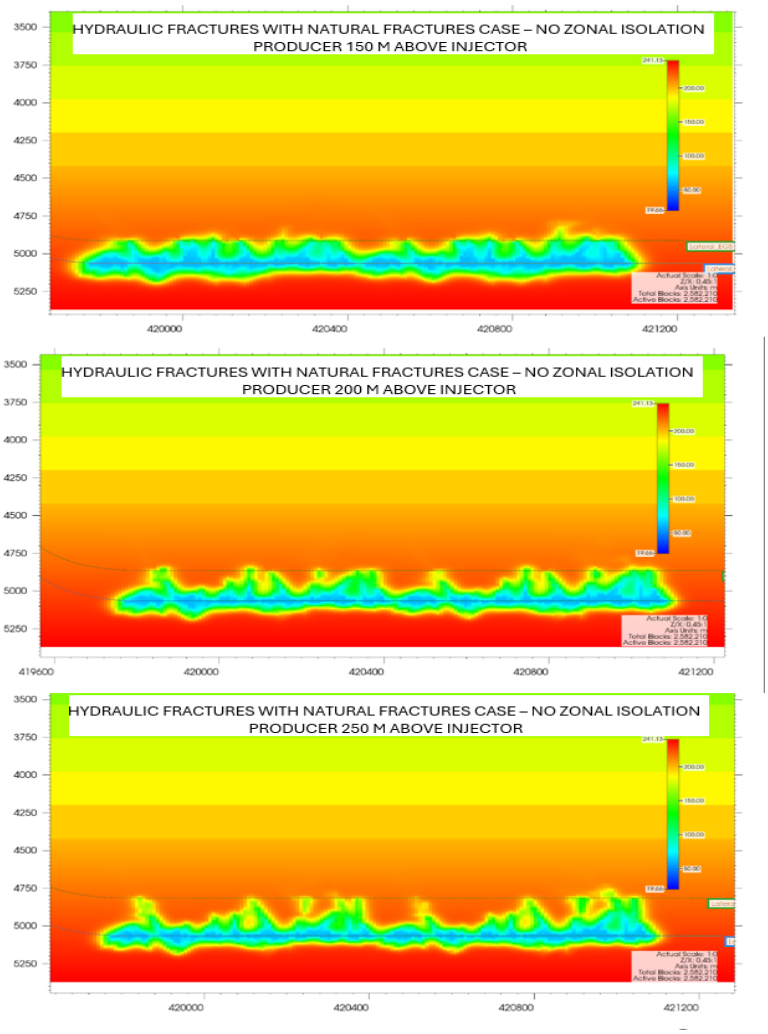

Figure 22. Reservoir temperature in the volume after 30 years of production for hydraulic fracture propagation within a preexisting natural fracture network without zonal isolation.

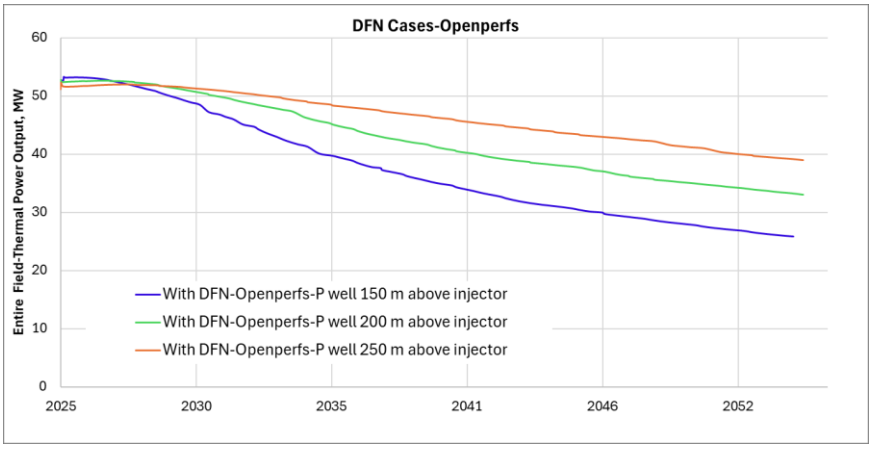

Figure 23. Decline curves over 30 years of production for hydraulic fracture propagation within a preexisting natural fracture network without zonal isolation.

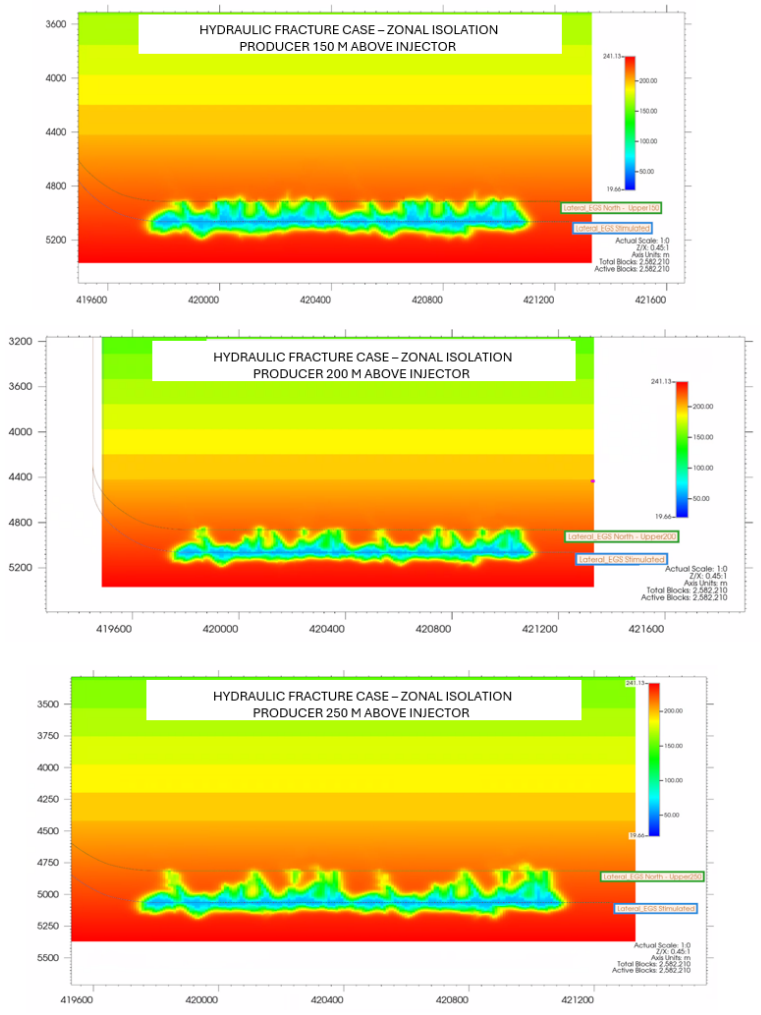

Figure 24. Reservoir temperature in the volume after 30 years of production for hydraulic fracture propagation within a preexisting natural fracture network with zonal isolation.

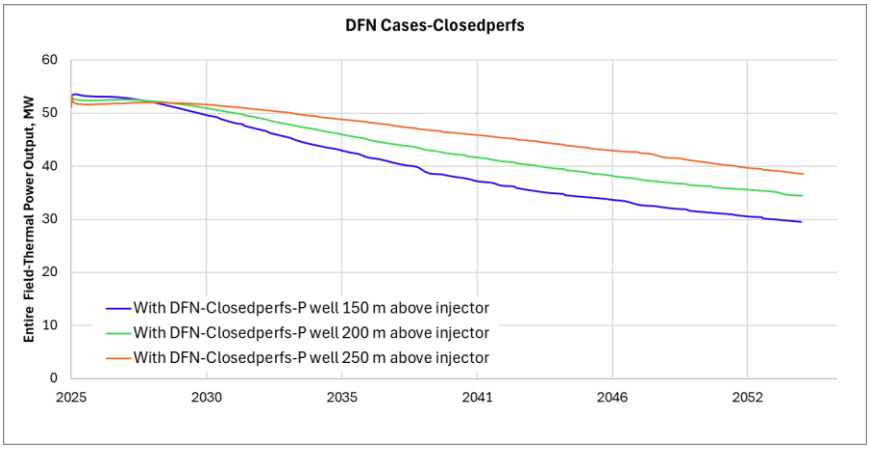

Figure 25. Decline curves over 30 years of production for hydraulic fracture propagation within a preexisting natural fracture network with zonal isolation.

Figures 26 summarizes these results for the 250 m well separation case on a single plot for comparison. Figure 27compares profiles of temperature along the production well for cases with and without natural fractures.

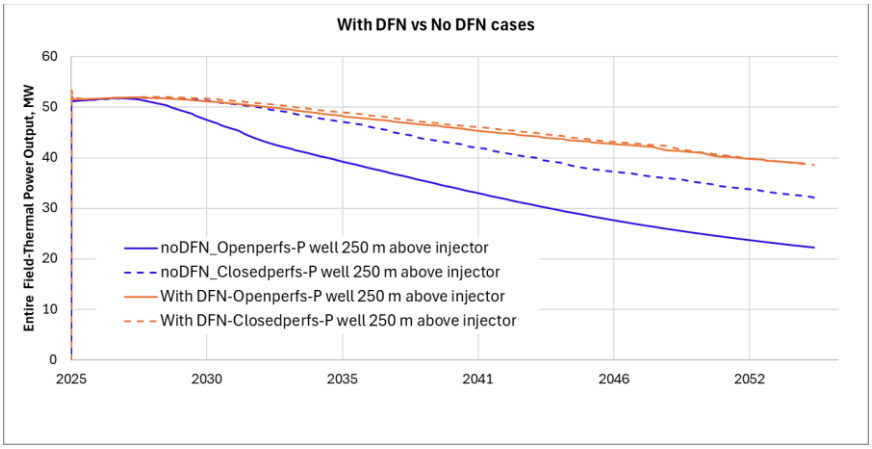

Figure 26. Summary of Decline curves over 30 years of production.

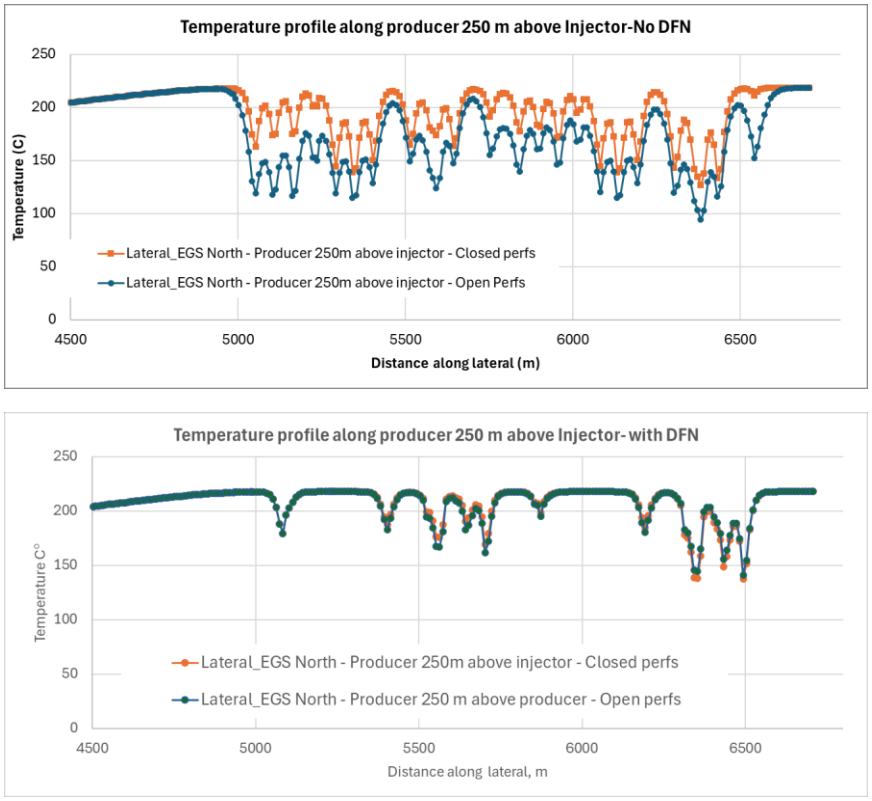

Figure 27. Temperature profile along the producer without (top) and with natural fractures (bottom).

4.3 Feasibility Economic Analysis

An economic assessment of selected geothermal development options based on full physics Dynamic Fracture Modeling was conducted to calculate the Levelized Cost of Electricity (LCOE) and Unit Overnight Capital Cost (OCC). The assessment uses the same economic and commercial assumptions described for the Pre-Feasibility Phase except for the well completions with and without zonal isolation. Cases 1and 2 compare hydraulic fracture propagation without natural fractures and with or without zonal isolation. For cases 3, 4, and 5, the injector is at a fixed depth and the producer is located at various distances above the injector. Cases 5 and 6 compare hydraulic fracture propagation through preexisting natural fractures with and without zonal isolation. The technical cases are listed in Table 2.

Table 2: Feasibility Cases for Economic Analysis

Site	Case	Technical Case for Economic Analysis
1	1	NO DFN ZONAL ISOLATION 250m ABOVE INJECTOR
1	2	NO DFN NO ZONAL ISOLATION 250m ABOVE INJECTOR
1	3	DFN ZONAL ISOLATION 150m ABOVE INJECTOR
1	4	DFN ZONAL ISOLATION 200m ABOVE INJECTOR
1	5	DFN ZONAL ISOLATION 250m ABOVE INJECTOR
1	6	DFN NO ZONAL ISOLATION 250 ABOVE INJECTOR

The relative Levelized Cost of Electricity (LCOE) values calculated using base case assumptions are shown in Figure 28. LCOE ranges are most sensitive to the completion with or without zonal isolation and next, to the location of the producer above the injector. Figure 29 is an example cost percent breakdown of the components of the LCOE for the hydraulic fracturing case with the producer 250m above the injector with zonal isolation.

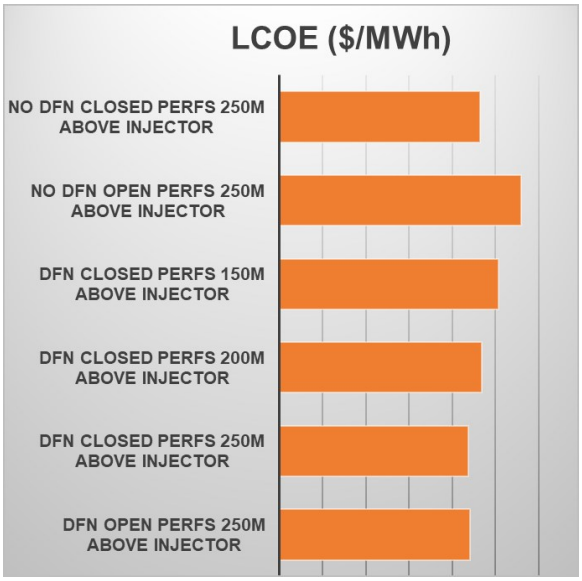

Figure 28. LCOE for cases shown in Table 2.

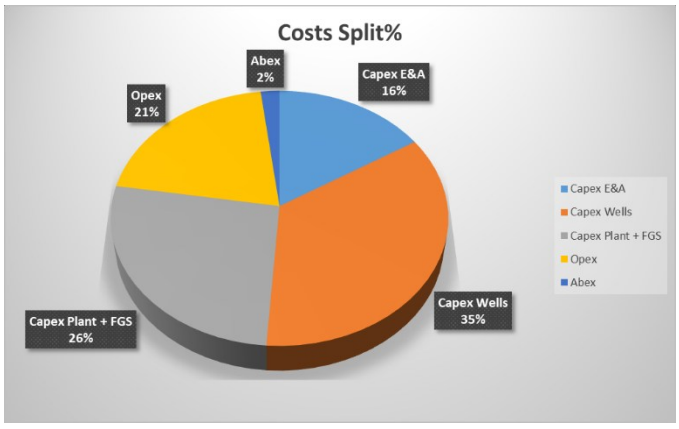

Figure 29. Example cost split for hydraulic fracturing for the case with the producer 250m above the injector with zonal isolation.

5. CONCLUSIONS

The workflow integrated structural and stratigraphic geomodeling, finite-element hydrostructural DFN simulations, and dynamic reservoir modeling to generate predictive 3D resource assessments. Economic feasibility was quantified through LCOE calculations, incorporating drilling, stimulation, and operational costs.

Technical analysis revealed naturally fractured systems as the most sustainable, achieving consistent energy production over a 30-year period under optimal fracture configurations. EGS scenarios exhibited variability in thermal output due to fracture density and cooling effects, with wider cluster spacing improving short-term efficiency but struggling with long-term thermal depletion in the absence of zonal isolation. Economically, naturally fractured reservoirs emerged as the most cost-effective (lowest LCOE). The study concludes that repurposing oil/gas sites for geothermal energy is viable in regions with high temperatures (>150°C) and natural fracture networks, with DFN-based systems offering the strongest technical and economic case for prioritization.

This work introduces an integrated workflow that uniquely combines reservoir modeling, fracture network simulation (DFN), Dynamic Fracture modeling (DFM), and economic analysis to assess geothermal potential at oil/gas sites—a novel contribution to both geothermal and petroleum literature. By providing comparative LCOE metrics it offers actionable benchmarks for industry decision-makers. Although the stochastic EGS modeling approach simplifies fracture simulation and reduces computational demands, far greater predictive accuracy is provided through full coupled thermo-hydro-mechanical modeling of the fracture networks (DFM) to simulate reservoir injection. Additionally, the findings highlight the advantage of stimulated naturally fractured reservoirs over hydraulically fractured massive rock masses in long-term geothermal projects, aligning with petroleum industry expertise in fracture management and infrastructure reuse. These insights bridge geothermal energy research with practical applications in the repurposing fossil fuel sites.

REFERENCES

Batir and Richards, Analysis of Geothermal Resources in Three Texas Counties, SMU Geothermal Laboratory, 2020. Research results for Task 5 of the Project: The Geothermal Entrepreneurship Organization (Geo) Accelerating Technology Transfer, Testing and Adoption of Cutting-Edge Extreme Environment Drilling, The University of Texas at Austin, DOE-GTO Prime Award: DE-EE0008971, Subaward number: UTA19-001356.

Barton, C., William Pettitt, W., Salter, T., Elena Meyer, E., Harper, C., Nasir, E., Moradi, A., Richard Alt, R., Likrama, F., Sims, D., Osborn, W., 2025. Next Generation Reservoir Modeling for Geothermal Energy and Lithium Recovery. PROCEEDINGS, 50th Workshop on Geothermal Reservoir Engineering, Stanford University, Stanford, California, February 10-12, 2025, SGP-TR-229

Blackwell, D., Richards, M., Frone, Z., Ruzo, A., Dingwall, R., & Williams, M., 2011. Temperature-At-Depth Maps for the Conterminous US and Geothermal Resource Estimates. GRC Transactions, 35 (GRC1029452)

Damjanac, B., M. Torres and C. Detournay. “Modeling the Effect of a Natural Fracture Network and Its Properties on Multi-Stage Stimulation,” in Proceedings, Unconventional Resources Technology Conference (URTeC, Houston, Texas, July 2021), URTeC: 5285. 2021.

Doe, T, McLaren, R., and Dershowitz, W. Discrete Fracture Network Simulations of Enhanced Geothermal Systems. PROCEEDINGS, Thirty-Ninth Workshop on Geothermal Reservoir Engineering, Stanford University, Stanford, California, (2014), SGP-TR-202

Ferrill, N., Ferrill, D., 2021. Influence of Mechanical Layering and natural fractures on undercutting and rapid headward erosion (recession) at Canyon Lakes Spillway, Texas, UDA. Engineering Geology, 280, Article 105897.

McCarthy, K. Pettitt, W., Engels, O., Priem, R., 2024. Geothermal Play Fairway Analysis (GPFA): A Texas/Gulf Coast Case Study. PROCEEDINGS, 49th Workshop on Geothermal Reservoir Engineering Stanford University, Stanford, California, February 12-14, 2024, SGP-TR-227

Moos, D and Barton, C., 2008. Modeling uncertainty in the permeability of stress-sensitive fractures. ARMA, Paper #:08-312.

Norbeck, J., Latimer, T., Gradl, C., Agarwal, S., Dadi, S., Eddy, E., Fercho, S., Lang, C., McConville, E., Titov, A., Voller, K., and Woitt, M., 2023. Review of Drilling, Completion, and Stimulation of a Horizontal Geothermal Well System in North-Central Nevada, PROCEEDINGS, 48th Workshop on Geothermal Reservoir Engineering Stanford University, Stanford, California, February 6-8, SGP-TR-224.Wang, C.T., and Horne, R.N.: Boiling Flow in a Horizontal Fracture, Geothermics, 29, (1999), 759-772.